



DWELL AND PENETRATION OF TUNGSTEN HEAVY ALLOY LONG-ROD PENETRATORS IMPACTING UNCONFINED FINITE-THICKNESS SILICON CARBIDE CERAMIC TARGETS

T. Behner, A. Heine¹ and M. Wickert

Fraunhofer EMI, Eckerstr. 4, 79104 Freiburg, Germany

Highlights

- We investigate protective properties of unconfined ceramic elements experimentally.
- Direct impact tests focus on the dwell potential of the finite-thickness ceramic.
- A bare ceramic tile can defeat a tungsten-alloy rod penetrator up to 900 m/s.
- A thin buffer layer on the ceramic shifts the threshold velocity up to 1700 m/s.
- Semi-infinite test results are confirmed for unconfined finite thickness ceramics.

Abstract

Impact experiments with a tungsten heavy alloy long rod projectile against silicon carbide tiles were performed to study the transition from dwell to penetration and to compare against earlier investigations which focused either on small scale semi-infinite set-ups or on finite thickness set-ups with confinement. A depth-of-penetration configuration consisting of a ceramic tile and an extended steel backing was used to assess the impact response of the unconfined finite-thickness ceramic. The ceramic tile was either bare or had a cover plate attached to the front. The cover plate thickness has been varied and gives best results for a

¹ Corresponding Author: andreas.heine@emi.fraunhofer.de Tel. +49 761 2714 435, Fax +49 761 2714 81435

thickness of about half the projectile diameter used in the experiments. For the bare ceramic, a long dwell phase can be maintained up to impact velocities of around 900 m/s. For the buffered ceramic, partial dwell can be achieved up to around 1700 m/s. The results corroborate those of earlier investigations mentioned above. More importantly, the present results show that it is possible to substantially erode a heavy alloy long-rod penetrator at the surface of a finite thickness ceramic element without lateral confinement in direct impact experiments even at high impact velocities.

Keywords: dwell, silicon carbide, long-rod projectile, impact experiments, mass efficiency.

Introduction

For the regime of long-rod penetrators impacting at velocities of about 1000 to 2000 m/s onto high-strength targets, the interaction behavior is strongly determined by material properties like strength and hardness [1]. This means, that contrary to the fully hydrodynamic regime, weight saving in protective structures is still possible by the application of low density materials as long as their compressive strength is sufficiently high. Therefore, it is a promising approach to use ceramic materials, although their brittleness gives rise to a complex behavior that requires appropriate design of protective elements.

Ceramics also exhibit a mechanism of defeating a projectile known as dwell effect or interface defeat: a high-velocity projectile erodes at the ceramic surface and flows out radially with no significant penetration (Figure 1). Dependent on material and target set-up, the duration of the dwell effect can vary from a fraction of the projectile interaction time up to a complete erosion of the projectile at the target surface. For the latter case, the term “interface defeat” is frequently used.

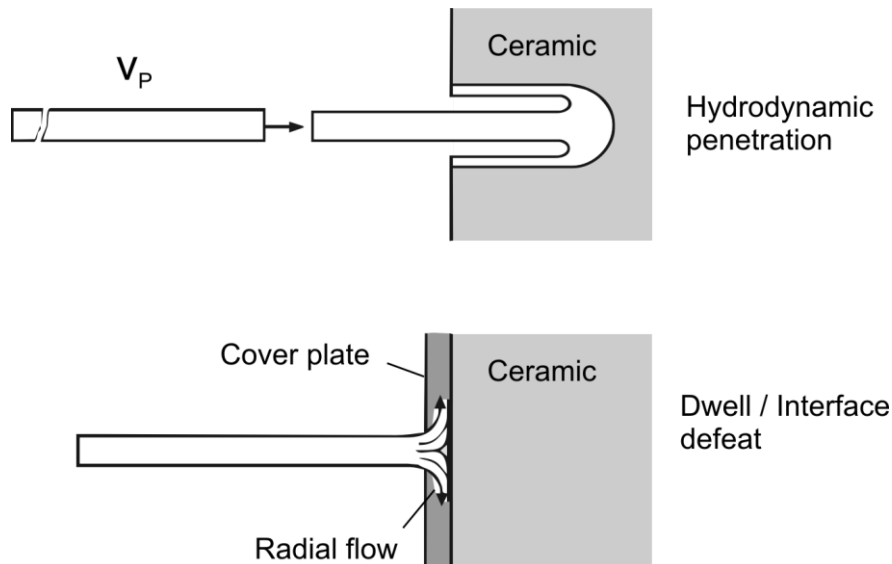


Figure 1: Principle of the dwell effect. Instead of penetrating into the target, the penetrator erodes at the target surface and flows out radially. The cover plate is optional and determines the transition velocity from dwell to penetration.

The dwell effect for rod penetrators has been investigated in complicated target arrangements about 15-25 years ago, e.g. [2]-[4], although the first observation of the basic effect in light armor studies dates back much earlier, e.g. [5]. As reviewed in [4], many different target layerings with light and heavy confinements were analyzed using direct-impact tests and also small-scale reverse impact tests. Nonetheless, due to the complexity inherent to the target design the key interaction mechanisms were still masked by the overall ballistic response of the setup. Therefore, a natural step was to consider bare and semi-infinite ceramics, in order to focus on the behavior of the ceramic material. This more academic approach also used small-scale reverse impact experiments and allowed for fundamental characterization of the ceramic material upon high-velocity impact of a long rod [6]-[13]. Lately, some in-depth theoretical analyses based partly on those small-scale results were also published [14]-[15].

In the present paper, we address the transferability of the results of the above work to direct impacts of tungsten heavy alloy (WHA) rod penetrators onto single ceramic tiles of limited thickness, only supported by a backing. This implies a significant increase in scale by a factor of 6 for key geometries like rod diameter compared to experiments done in, e.g., [12]-[13] and at the same time a reduction of the thickness of the ceramics to less than 5 times the projectile diameter, i.e. we aim at extending prior work, e.g. [12] and [13], to completely different parameter ranges and at corroborating the transferability of well-known basic effects to different dimensions by experimental evidence.

Experimental Set-Up

The W-Ni-Fe based generic tungsten-heavy-alloy (WHA) penetrator used in the experiments has a diameter D of 6 mm and a length L of 90 mm. The 9 mm long nose section is conical with a 3.6 mm blunt tip (see Figure 2). The penetrator material is Kennametal E-922Y. The ceramic targets are quadratic tiles of dimensions 100 mm x 100 mm, 25 mm thick, made of commercial grade, pressureless sintered silicon carbide (SiC). The specific material is designated as SiC-F and is manufactured by 3M (formerly EKasic-F from ESK). A target consists of one SiC tile glued to a rolled homogenous armor (RHA) steel plate of 40 mm thickness. Depending on the impact velocity, additional RHA plates are placed behind the target, in order to ensure a semi-infinite RHA target for penetration measurement. Table 1 shows the key mechanical properties for the different materials.

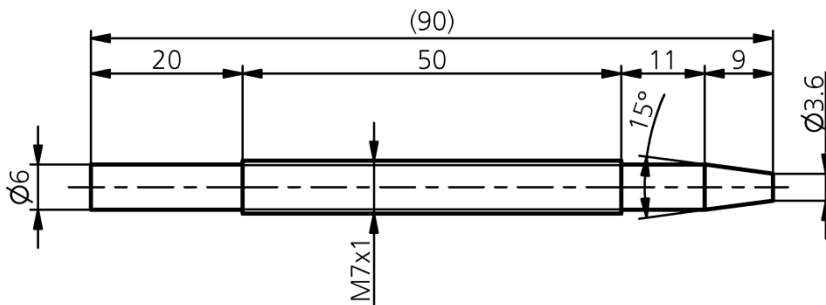


Figure 2: Penetrator dimensions.

The sabot-guided projectile was accelerated with a powder gun into a stationary observation tank. The impact was monitored with a multiple anode X-ray tube and a high-speed video camera. The impact velocity was varied between 400 and 1800 m/s. Experiments were carried out for the bare ceramic and for a buffered version, where a small copper disc was glued to the ceramic surface (see Figure 3). The purpose of the copper buffer is to attenuate the impact shock and to increase the dwell-to-penetration transition velocity compared to a bare surface. The basic effect of such buffers is well-known as, .e.g., discussed in [2], [8], [16], or [17]. The buffer thickness was optimized at a constant impact velocity followed by a variation of the velocity for the optimal buffer thickness. Contrary to prior work [17], the buffer thickness identified as reasonable in the present work is smaller than the projectile diameter. Also, unlike in [16], the buffer is not combined with lateral confinement.

Table 1: Key mechanical properties.

Material	WHA	SiC	RHA	Cu
Source	Certificate	Datasheet	Specification	Datasheet
Density [g/cm ³]	17.6	> 3.15	7.85	8.9
Ultimate Tensile Strength [N/mm ²]	1360	-	900	~270
Elongation at Fracture [%]	10	-	12	~20
Hardness	475 HV 10	2650 HV 0.5	280-330 HBW	~80 HB
Elastic Modulus [GPa]	-	430	-	-
Flexural Strength [GPa]	-	400	-	-
Compressive Strength [GPa]	-	> 2500	-	-
Fracture Toughness [MPa m ^{0.5}]	-	4	-	-

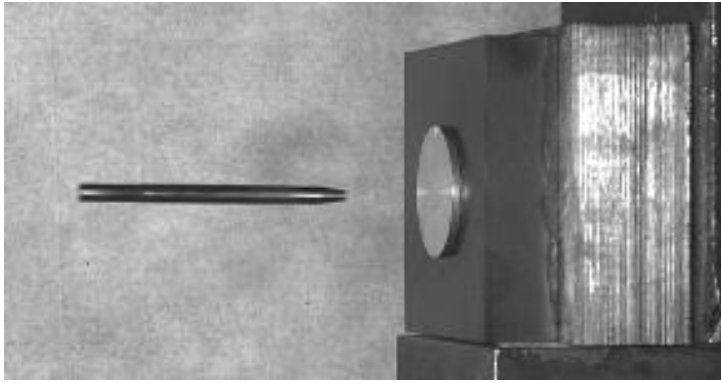


Figure 3: Frame from high-speed video, showing the experimental set-up inside the impact tank prior to the projectile impact.

Experimental Results

Table 2 shows the results for the bare ceramic targets (9 experiments). Total yaw angle, impact velocity v_P and residual penetration depth P_R into the supporting RHA plates were measured. The area density of the penetrated material for the complete target arrangement calculates as

$$\rho_A = \rho_{SiC} \cdot l_{SiC} + \rho_{RHA} \cdot P_R \quad (1)$$

from the densities ρ_{SiC} and ρ_{RHA} of ceramic and backing, respectively, the thickness of the ceramic l_{SiC} and the residual penetration in the backing P_R . The standard velocity measurement procedure yields an error of about 1 %. The error for the depth measurement is about ± 0.1 mm.

Table 2: Experimental results for the bare ceramic target.

Test #	Exp.	Yaw [°]	v _P [m/s]	P _R [mm]	ρ _A [kg/m ²]
1	13057	1.0	380	0.4	83.1
2*	13053	0.9	525	1.7	93.3
3	13048	1.3	593	1.1	88.6
4	13043	1.3	773	4.8	117.7
5	13044	2.5	891	6.6	131.8
6	13047	0.9	988	12.7	179.7
7	13045	0.5	1205	28.9	306.9
8*	13059	0.3	1356	35.2	356.3
9	13046	1.5	1525	45	433.3

* Tests specifically discussed in the text

Results for the buffered target configurations are given in Table 3 (8 experiments). In addition to the data of Table 2 the buffer thicknesses l_{Cu} is incorporated. Accordingly, the area density of the penetrated material for the buffered target arrangement calculates with the density ρ_{Cu} of the buffer as

$$\rho_A = \rho_{Cu} \cdot l_{Cu} + \rho_{SiC} \cdot l_{SiC} + \rho_{RHA} \cdot P_R \quad (2)$$

Table 3: Experimental results for the buffered ceramic target.

Test #	Exp.	Yaw [°]	v _P [m/s]	l _{Cu} [mm]	P _R [mm]	ρ _A [kg/m ²]
10	13049	0.9	1194	3	14.9	223.7
11	13050	1.3	1203	4	14.9	232.6
12	13051	1.1	1211	6	23.8	320.2
13	13054	2.0	1200	1.5	17.4	230.0
14*	13055	1.8	1019	3	6.8	160.1
15*	13056	0.7	1678	3	15.9	231.5
16	13058	0.4	1478	3	19.5	259.8
17	13060	1.5	1837	3	62.4	596.5

* Tests specifically discussed in the text

Flash X-ray observation

Figure 4 compares the flash X-ray pictures of two different impact velocities for the bare and the buffered target. For the bare target of Test 2 at a v_P of around 500 m/s, penetrator fragments are visible on the target surface and show the radial flow behavior characteristic of the dwell effect. At a higher v_P of around 1350 m/s (Test 8), no penetrator fragments are

visible on the ceramic surface. The rod penetrates the ceramic and the RHA plate. Due to the lateral dimensions of the ceramic, the X-ray radiation is fully absorbed and the penetration process itself is not visible in these images.

In case of the buffered target, the copper buffer (3 mm thickness) shows a bulging during the impact process with slightly different shapes for the different impact velocities (around 1000 m/s for Test 14 and around 1700 m/s for Test 15). The copper shields the X-ray radiation, thus no penetrator fragments are visible. The bulging suggests that there is material expanding radially below the buffer plate, similar to the material flow clearly visible in case of the bare ceramics in test 2.

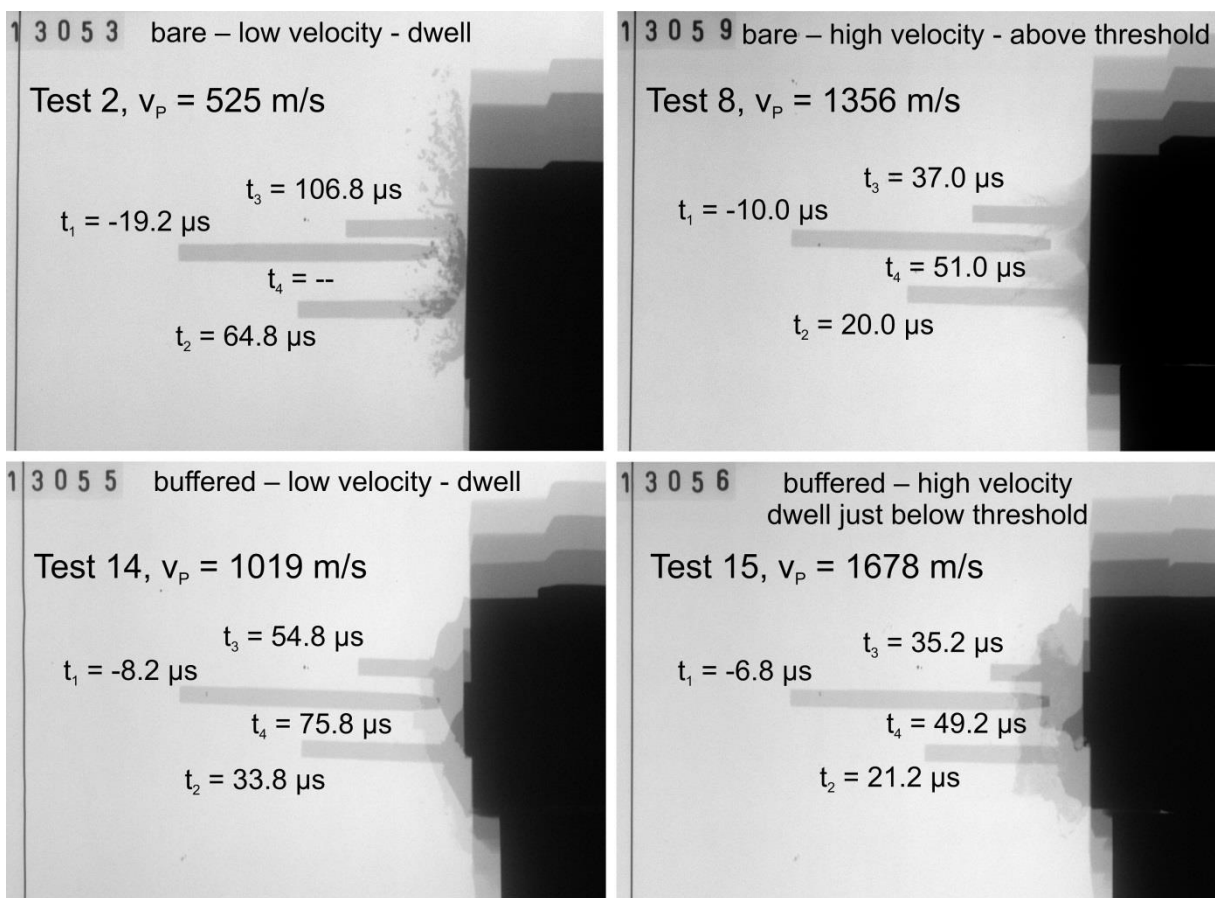


Figure 4: Four-fold flash X-ray pictures for the bare target (Tests 2 and 8, upper row) and the buffered target (Tests 14 and 15). t_1 to t_4 indicate the calculated times before/after impact.

Crater Phenomenology

Figure 5 shows the corresponding crater images of the cross-sectioned RHA plates for the tests of Figure 4. For the bare targets of Test 2 (dwell) and 8 (penetration), the difference in penetration depth is significant and reflects the 850 m/s difference in v_p . For the buffered targets of Tests 14 and 15, the penetration depth is smaller than in test 8. Apparently, the

penetrator dwells at a v_p of around 1700 m/s for a substantial time (Test 15). At a significantly reduced v_p of around 1000 m/s (Test 14), the penetration depth is only slightly smaller as for Test 15. It seems that the dwell effect is less distinct at the lower velocity.



Figure 5: Crater images for the bare target (Tests 2 and 8) and the buffered target (Tests 14 and 15)

High-speed videos

For the four tests discussed before, Figure 6 shows a sequence of three images each from a high-speed video, which represent approximately the three X-ray times t_2 to t_4 after impact indicated in the corresponding flash X-ray for the specific test. Generally, detailed phenomena of the dwell effect, like projectile fragments, are obscured by dust and light reflections.

Nonetheless, some interesting effects are visible. For the bare targets, the interaction of the projectile with the ceramic differs significantly for the lower and the higher impact velocity. Whereas for Test 2, a radial particle expansion almost parallel to the ceramic surface is clearly visible, Test 8 shows a backwards oriented funnel-shaped particle expansion. This is similar to a phenomenon observed recently in the hypervelocity impact onto a different type of brittle, but low-strength, material of similar density [18].

For the tests with buffer, the bulging of the copper plate visible in the X-ray images is also seen in the optical images.

In addition, the development of cracks is visible for the ceramic target. As the interaction time of the penetrator with the ceramic is longer at lower impact velocities, the images at t_4 show a

later point in time and thus more developed cracks for Tests 2 and 14 than for Tests 8 and 15, respectively. However, comparing images for each case taken at nearly 300 μ s after impact, when the penetrator either is consumed or has penetrated the steel backing, it becomes evident that for the lower impact velocities, overall damage of the ceramic is substantially lower than for the higher velocities (Figure 7).

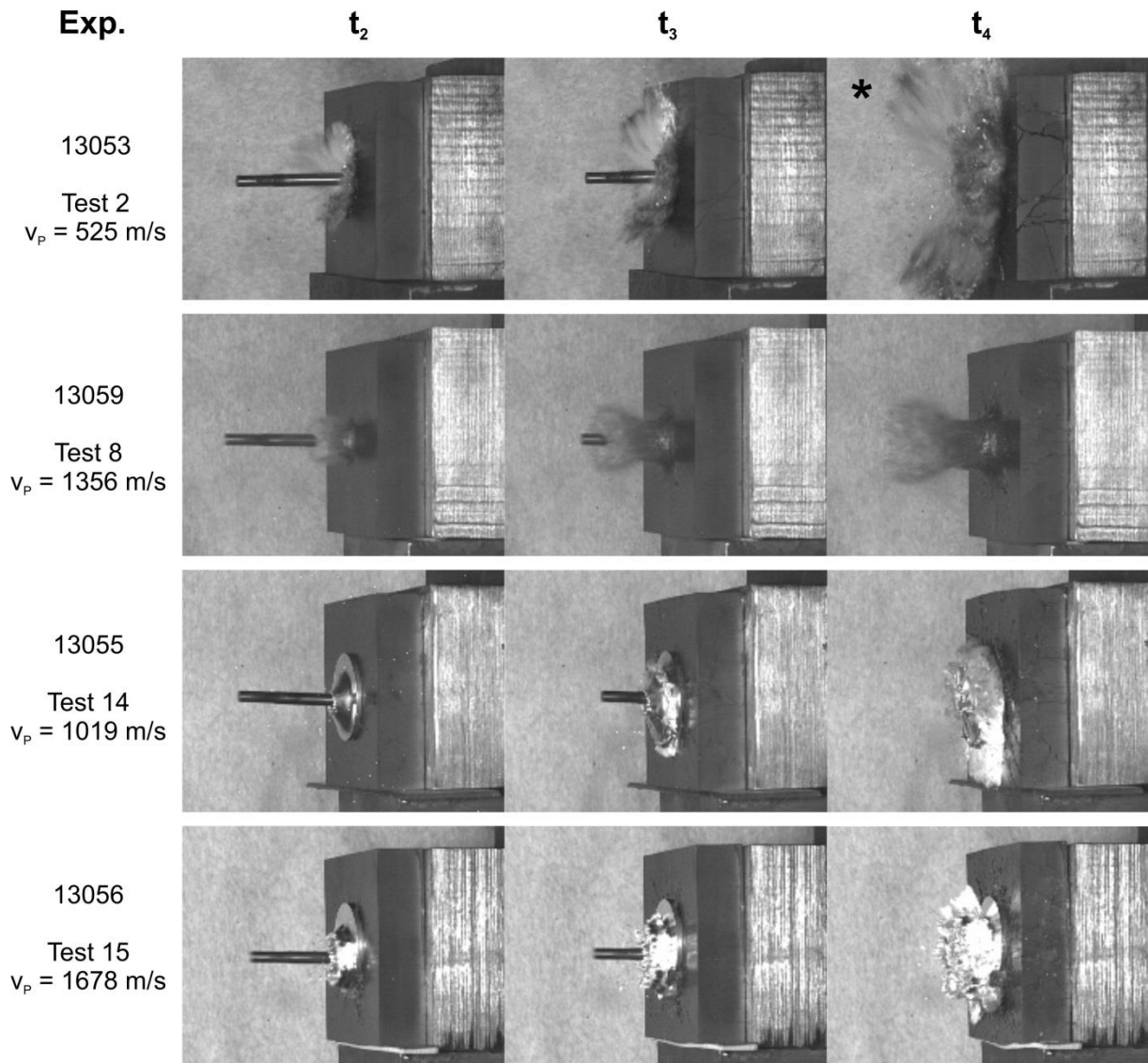


Figure 6: High-speed video images corresponding approximately to the indicated X-ray times in Figure 4. (*) Note that for Test 2, no X-ray picture at t_4 exists.

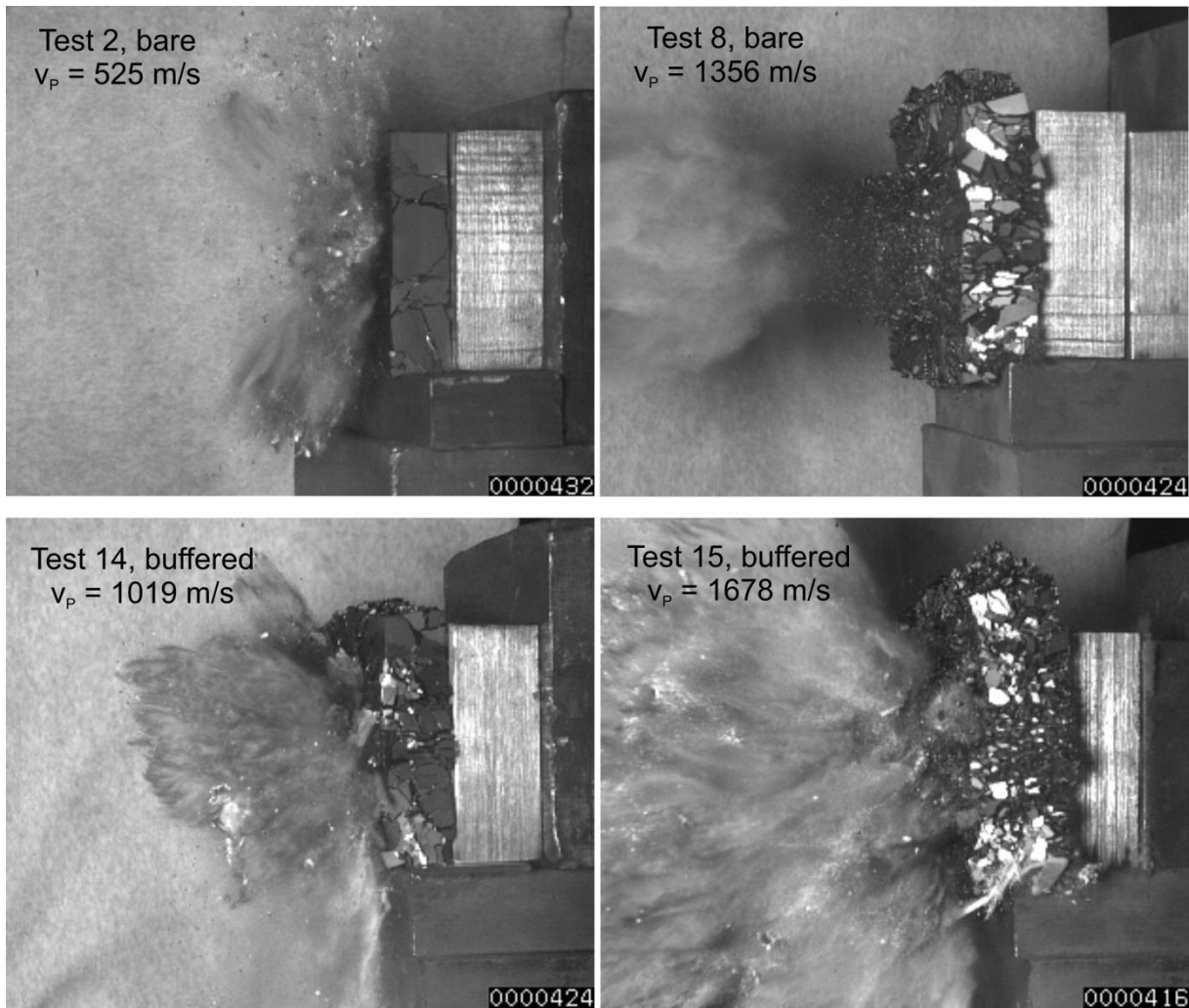


Figure 7: High-speed video images taken at around 300 μ s after impact.

Evaluation of Dwell and Penetration

Figure 8 shows the area density of the penetrated material ρ_A versus impact velocity v_P for the various experiments. Additionally, penetration into semi-infinite RHA is shown according to the Walker –Anderson model for penetration [19]. Main parameters for WHA and RHA were taken from Table 1. The strength parameter of RHA had to be increased in the model (to 1.3 GPa) to match data for the semi-infinite reference penetration of the penetrator into RHA of representative quality (diamond symbols), see also Table 4. Note, however, that the target strength in the Walker –Anderson model represents an effective flow stress, which is typically larger than given by quasi-static measurements [20].

Table 4: Reference penetration of the penetrator into semi-infinite RHA, exemplary data from [21].

Test #	Exp.	Yaw [°]	v_P [m/s]	P [mm]	ρ_A [kg/m ²]
Ref-1	12617	2.6	1250	44.5	349.3
Ref-2	12627	1.0	1560	73.4	576.2
Ref-3	12621	1.3	1770	91.7	719.8

For the bare ceramic targets (square red data points) up to $v_P = 900$ m/s the total penetration is almost constant. This corresponds to a fragmentation of the ceramic layer without more than superficial penetration into the RHA backing as well as to the indications of the dwell effect that are visible in the X-ray images obtained for those experiments. However, as the steel backing nonetheless shows small indentions for all of those experiments, it is evident that the penetrator dwells only partially and does not completely erode at the surface and during the subsequent penetration of the ceramic. For v_P above 900 m/s the total penetration increases linear with impact velocity.

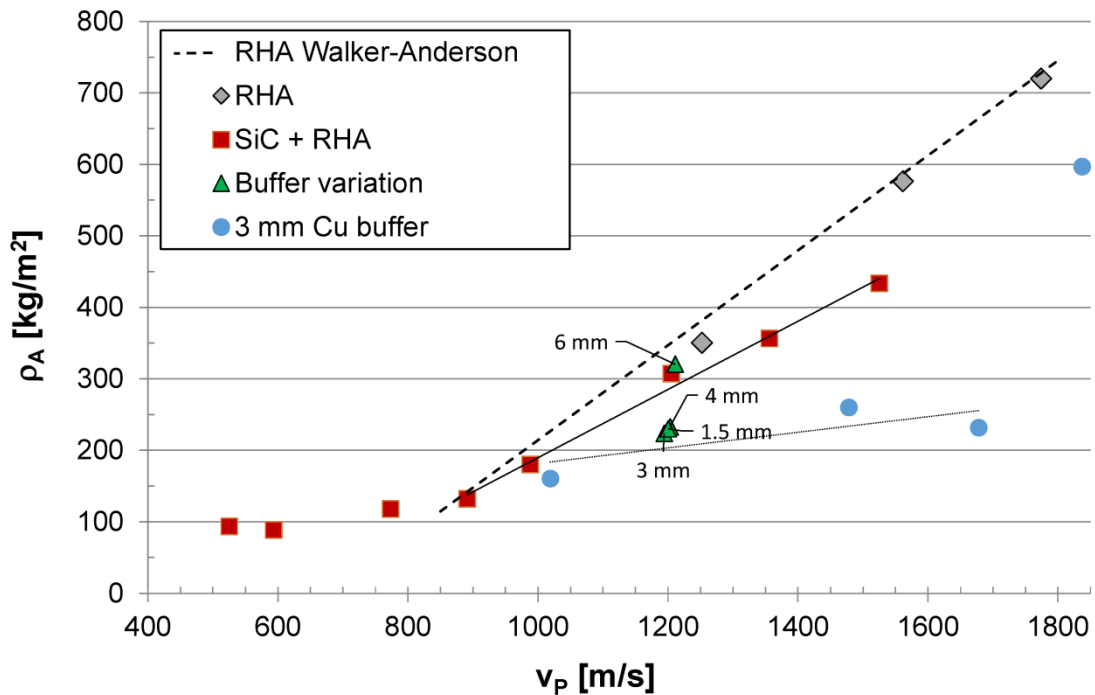


Figure 8: Area density ρ_A of penetrated material (complete target arrangement) versus impact velocity v_P .

For the buffered targets, the first step was a variation in buffer thickness from 100% down to 25 % of the projectile diameter at a constant v_P of about 1200 m/s to see the effects on overall

target performance (triangular symbols). While the 4, 3 and 1.5 mm buffer configurations perform similar and exhibit a lower ρ_A than the bare target configuration, the 6 mm buffer configuration achieves only about the same ρ_A as the bare target (Figure 9). This is an indication that a thick buffer may inhibit the dwell potential of the ceramic. As the 3 mm buffer shows the lowest ρ_A values of all tested buffer configurations, it was chosen for all subsequent tests where v_P was varied.

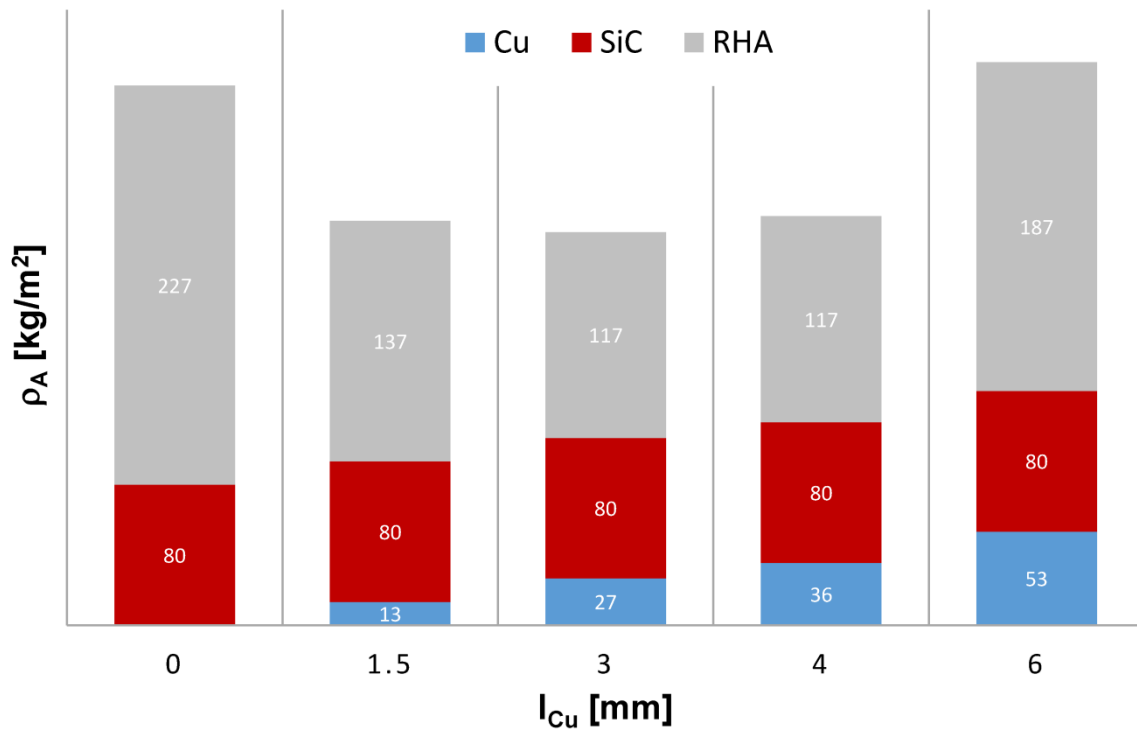


Figure 9: Area density ρ_A of penetrated material (specified for each material of target arrangement) at around 1200 m/s impact velocity for the different buffer configurations (buffer thickness l_{Cu}). There is a minimum around $l_{Cu} = 3$ mm, i.e. for a buffer thickness that is one half of the projectile diameter. Such thin buffers had not been used in the investigations of, e.g., [9], [10], [12], or [13].

Considering in the following the tests with the 3 mm buffer only (Figure 8 – round symbols) the penetrated area density remains in the range of 150 kg/m² up to 270 kg/m² and thus a substantial erosion of the heavy alloy long rod penetrator by partial dwell occurs when compared to the penetration values for the bare target. The difference in ρ_A between buffered and bare target increases with impact velocities of up to 1700 m/s.

At around 1800 m/s though, the difference in ρ_A between buffered and the linear extrapolation for the bare target becomes very small. Here, v_P is well above the transition velocity from

dwell to penetration for a similar material combination investigated in [9]. Therefore, penetration is expected to start right away with no dwell phase.

Overall, the results correspond well to findings in the literature [22]-[25] where dwell and the transition from dwell to penetration are closely linked to the material properties of target and penetrator.

Experiments with buffered finite thickness SiC targets at different scales presented in [26] show a transition from complete dwell to penetration at around 1000 m/s for dimensions comparable to those of the present study (rod diameter 5 mm – target length 50 mm) and direct impact conditions. However, the copper buffer element is four times thicker than the rod diameter. As shown above with the buffer variation this can cause a reduction in overall target performance.

Mass efficiency of the ceramic target

The total mass efficiency E_M of the ceramic target is defined as ρ_A (penetrated area density) of the semi-infinite RHA divided by ρ_A of the respective complete target arrangement consisting of ceramics, backing, and optional buffer. Figure 8 shows that for impact velocities v_P above 900 m/s, there is a linear increase of the total penetration with impact velocity for RHA and the bare ceramic target. To a lesser extent, a linear increase can also be assumed for the buffered ceramic target up to a v_P of around 1600 m/s. Interestingly, the three linear curves of different slopes intersect at around $v_P = 900$ m/s, i.e. at that velocity the mass efficiency of ceramics (bare and buffered) with RHA backing is about 1 in relation to RHA. At higher impact velocities – i.e. in between 900 m/s and 1600 m/s – the mass efficiency increases by a nonlinear function determined by the different slopes of the linear curves for ρ_A and their common offset of about 100 kg/m^2 at around $v_P = 900$ m/s. Figure 10 shows the total mass efficiency E_M in relation to RHA for the bare and buffered ceramic target as a function of v_P . In the considered velocity range of 900 m/s to 1600 m/s, E_M for the bare target increases only slightly from 1 up to 1.3. However, E_M for the buffered target arrangement increases significantly from 1 up to 2.5. So the buffer not only increases the transition velocity from dwell to penetration but has also a positive effect on the mass efficiency of the target.

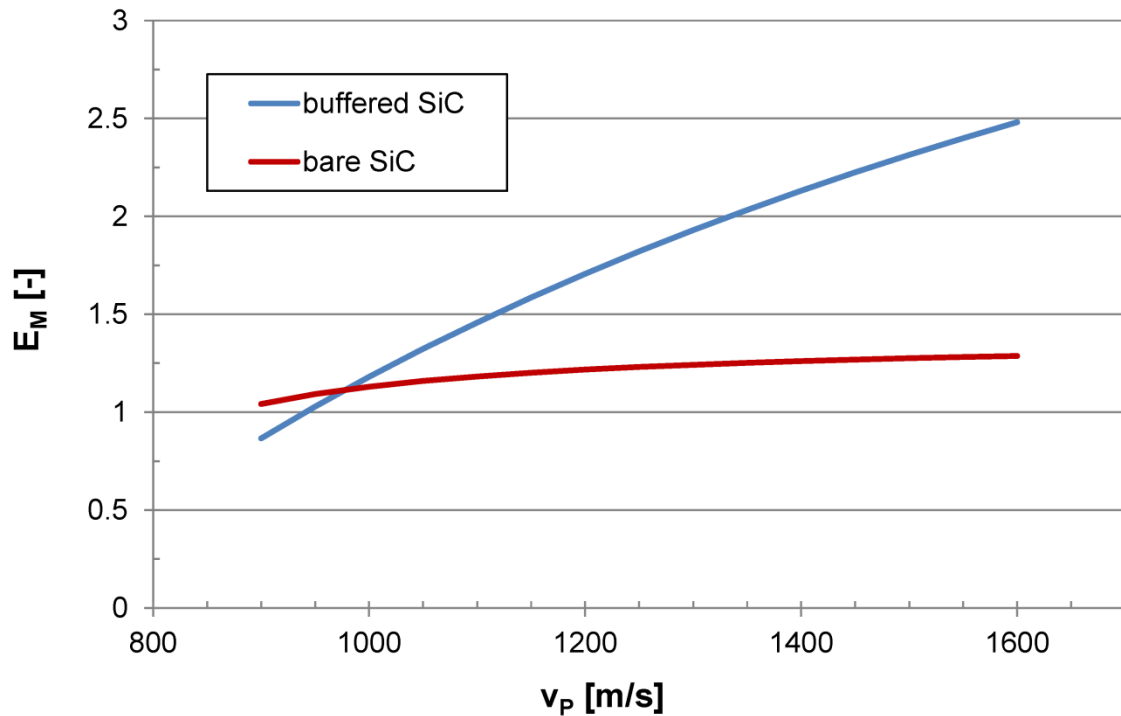


Figure 10: Mass Efficiency E_M in relation to RHA versus impact velocity v_P . The curves are based on the linear fits in Figure 8.

Conclusions

To extend and verify findings in material behavior with respect to the dwell effect on ceramics - so far derived mainly from experiments with semi-infinite or confined ceramic samples - direct impact experiments with long WHA rods against unconfined, finite thickness SiC tiles supported by a steel backing were performed at impact velocities ranging from 500 m/s to 1800 m/s. The simple test set-up with significantly increased dimensions compared to earlier work focuses on the dwell potential of the finite-thickness ceramic and thus avoids considering the complicated interplay of a ceramic element with its confinement and the applied pre-stresses in set-ups that are commonly found in literature.

The new experiments show that at least a partial dwell effect for heavy alloy long-rod penetrators at laboratory-scale can be achieved without a complicated target set-up for finite-thickness ceramics, even without lateral confinement. A buffer material in front of the ceramic that attenuates the impact shock can increase the transition velocity as well as the mass efficiency of the target. The variation in buffer layer thickness showed that the best protective properties are achieved for a layer thickness of about half of the thickness of the laboratory penetrator diameter.

The results show that it is possible to substantially erode a heavy alloy long-rod penetrator at the surface of a finite thickness ceramic element even without lateral confinement. This has been proven by direct impact experiments at impact velocities up to 1700 m/s.

Acknowledgements

We acknowledge the financial support by the German Federal Ministry of Defence (BMVg) and The Federal Office of Bundeswehr Equipment, Information Technology and In-Service Support (BAAINBw).

References

- [1] Hohler V, Stilp A, Long-rod penetration mechanics. In: Zukas JA. High velocity impact dynamics. John Wiley and Sons, New York: 1990. pp. 321-404
- [2] Hauver GE, Netherwood PH, Benck RF, Kecskes LJ. Ballistic performance of ceramic targets. Army Symposium on Solid Mechanics, Plymouth, MA, 17-19 August, 1993.
- [3] Espinosa HD, Brar NS, Yuan G, Xu Y, Arrieta V. Enhanced ballistic performance of confined multi-layered ceramic targets against long rod penetrators through interface defeat. *Int. J. of Solids and Structures*. 2000; 37: 4893-4913.
- [4] Hauver GE, Rapacki Jr. EJ, Netherwood PH, Benck RF. Interface defeat of long-rod projectiles by ceramic armor. Army Research Laboratory, Report ARL-TR-3590, September 2005.
- [5] Wilkins ML, Cline CF, Honodel CA. Fourth Progress Report of Light Armor Program. Lawrence Radiation Laboratory, University of California, Livermore, Report UCRL-50694, June 1969.
- [6] Lundberg P, Renstrom R, Lundberg B. Impact of metallic projectiles on ceramic targets: transition between interface defeat and penetration. *Int. J. Impact Eng*. 2000; 24(3): 259-275.
- [7] Lundberg P, Renstrom R, Holmberg L. An experimental investigation of interface defeat at extended interaction time. In: Proc. 19th Int. Symp. Ballistics, Interlaken,

Switzerland, 2001, vol 3. , pp. 1463-1469, reprints available from International Ballistics Society, contact: president@ballistics.org

- [8] Holmquist TJ, Anderson Jr. CE, Behner T. Design, analysis and testing of an unconfined ceramic target to induce dwell. In: Proc. 22nd Int. Symp. Ballistics, Vancouver, Canada, 2005, vol. 2 , pp. 860-868 (DEStech Publication, Lancaster, PA, USA, 2005).
- [9] Lundberg P, Lundberg B. Transition between interface defeat and penetration for tungsten projectiles and four silicon carbide materials. *Int. J. Impact Eng.* 2005; 31(7): 781-792.
- [10] Lundberg P, Renstrom R, Lundberg B. Impact of conical tungsten projectiles on flat silicon carbide targets: transition from interface defeat to penetration. *Int. J. Impact Eng.* 2006; 32(11): 1842-1856.
- [11] Andersson, O, Lundberg P, Renstrom R. Influence of confinement on the transition velocity of silicon carbide. In: Proc. 23rd Int. Symp. Ballistics, Tarragona, Spain, 2007, vol 2. , pp. 1273-1280, reprints available from International Ballistics Society, contact: president@ballistics.org
- [12] Behner T, Anderson Jr. CE, Holmquist TJ, Wickert M, Templeton DW. Interface defeat for unconfined SiC ceramics. In: Proc. 24th Int. Symp. Ballistics, New Orleans, LA, USA, 2008, vol. 1, pp. 35-42 (DEStech Publications, Lancaster, PA, USA, 2008).
- [13] Behner T, Anderson Jr. CE, Holmquist TJ, Orphal DL, Wickert M, Templeton DW. Penetration dynamics and interface defeat capability of silicon carbide against long rod impact. *Int. J. Impact Eng.* 2011; 38(6): 419-425.
- [14] Li JC, Chen XW, Ning W. Comparative analysis on the interface defeat between the cylindrical and conical-nosed long rods. *Int. J. Protective Structures.* 2014; 5 (1): 21-46.
- [15] Li JC, Chen XW, Ning W, Li XL. On the transition from interface defeat to penetration in the impact of long rod onto ceramic targets. *Int. J. Impact Eng.* 2015; 83: 37-46.
- [16] Pickup IM, Barker AK, Elgy, ID, Peskes GJJM, van de Voorde M. The effect of coverplates on the dwell characteristics of silicon carbide subject to KE impact. In: Proc. 21st Int. Symp. Ballistics, Adelaide, Australia, 2004, vol. 2, pp. 207-213, reprints available from International Ballistics Society, contact: president@ballistics.org

- [17] Holmquist TJ, Anderson CE, Behner T. The effect of a copper buffer on interface defeat. In: Proc. 24th Int. Symp. Ballistics, New Orleans, LA, USA, 2008, vol. 2, pp. 721-728 (DEStech Publications, Lancaster, PA, USA, 2008).
- [18] Hoerth T, Schäfer F, Thoma K, Kenkmann T, Poelchau MH, Lexow B, Deutsch A. Hypervelocity impacts on dry and wet sandstone: Observations of ejecta dynamics and crater growth. *Meteoritics and Planetary Science*. 2013; 48 (1): 23-32.
- [19] Walker JD, Anderson Jr. CE, A time dependent model for long-rod penetration. *Int. J. Impact Eng.* 1995; 16(1): 19-48.
- [20] Riegel JP, Anderson Jr. CE, Target effective flow stress (EFS) calibrated using the Walker-Anderson penetration model. In: Proc. 28th Int. Symp. Ballistics, Atlanta, GA, USA, 2014, vol. 2, pp. 1242-1252 (DEStech Publications, Lancaster, PA, USA, 2014).
- [21] Frueh P, Heine A, Weber KE, Wickert M. Effective depth-of-penetration range due to hardness variation for different lots of nominally identical target material. *Defence Technology* 2016; 12(2): 172-177.
- [22] Hilton CD, McCauley JW, Swab JJ, Shanholtz ER, Portune AR. Quantifying bulk plasticity and predicting transition velocities for armor ceramics using hardness indentation tests. Army Research Laboratory, Report ARL-TR-6050, July 2012.
- [23] Jaansalu KM. Material properties and interface defeat. In: Proc. 27th Int. Symp. Ballistics, Freiburg, Germany, 2013, vol. 2, pp. 1277-1288 (DEStech Publications, Lancaster, PA, USA, 2013).
- [24] Behner T, Heine A, Wickert M. Protective properties of finite-extension ceramic targets against steel and copper projectiles. In: Proc. 27th Int. Symp. Ballistics, Freiburg, Germany, 2013, vol. 2, pp. 1598-1607 (DEStech Publications, Lancaster, PA, USA, 2013).
- [25] Aydelotte B, Schuster B, Impact and penetration of SiC: The role of rod strength in the transition from dwell to penetration. *Proc. Eng.* 2015; 103: 19-26.
- [26] Lundberg P, Renström R, Andersson O. Influence of length scale on the transition from interface defeat to penetration in unconfined ceramic targets. *J. Appl. Mech.* 2013, 80 (3): 031804-031804-9.